

Comparison between MAP and post-processed ML for incorporating anatomical knowledge in emission tomography.

Johan Nuyts, *Member, IEEE*, Kristof Baete, *Student Member, IEEE*, and Patrick Dupont

Abstract— Previously, the noise characteristics obtained with maximum-a-posteriori (MAP) reconstruction have been compared to those obtained with post-smoothed maximum-likelihood (ML) reconstruction, for applications requiring uniform resolution. It was found that MAP-reconstruction was not superior to post-smoothed ML. In this study a similar comparison is made, but now for applications where the noise suppression is tuned with anatomical information. Our first findings indicate that for these applications, MAP-reconstruction outperforms post-processed ML reconstruction.

I. INTRODUCTION

In previous studies, the noise performance of post-smoothed maximum-likelihood (ML) reconstruction has been compared to that of penalized-likelihood reconstruction, for emission tomography applications requiring “uniform” spatial resolution [1], [2]. Here, resolution is considered uniform if the local impulse response has spherical symmetry and is independent of the object and of the position in the image. The results indicated that noise suppression with penalized-likelihood is not superior to that with post-smoothed ML for these applications.

There is an increasing interest in the combination of anatomical and functional information. Promising results have been obtained with MAP-reconstruction, by using the anatomical information to modify the prior as a function of position. With this approach, the resulting resolution is strongly position and orientation dependent. In this work, we study the noise characteristics obtained with maximum-a-posteriori (MAP) reconstruction using anatomical priors, with those obtained with post-processing the ML reconstruction.

II. METHODS

A simulation study was performed using the Shepp-Logan phantom (figure 1). The phantom consists of 3 different anatomical components, each with its own uniform activity (relative activities of 3, 1, and 0). The reconstructions are used for the detection of regionally decreased tracer uptake in the most active component (the analogue of the gray matter in PET-FDG brain studies). The study uses the “signal known exactly, background known exactly” assumption, where presence or absence of a known signal must be detected in a

Work supported by K.U.Leuven grants IDO-99/005, OT-00/32 and F.W.O. grant G.0174.03.

Nuclear Medicine, K.U.Leuven, B-3000 Leuven, Belgium. (e-mail: Johan.Nuyts@uz.kuleuven.ac.be)

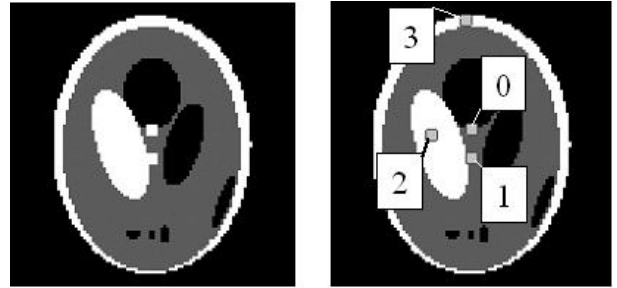


Fig. 1. Shepp-Logan phantom, consisting of 3 different anatomical components. In one of these, four regions are used to measure the signal-to-noise ratio for the detection of a 20% decrease in tracer uptake.

known background in the presence of noise [3]. Five noise-free sinograms were computed (100 detectors x 144 angles): one with normal activity everywhere, and one with a 20% decreased activity in each of the four regions. Attenuation was ignored, and detector resolution was assumed to be ideal, except for the blurring due to the projector/backprojector.

If no a-priori knowledge is available, the ideal observer computes a statistic H_0 from the sinogram data as follows:

$$H_0 = (\bar{Y}_1 - \bar{Y}_0)^t K^{-1} Y, \quad (1)$$

where \bar{Y}_1 and \bar{Y}_0 are the expected sinograms in the presence and absence of the signal, K is the covariance matrix and Y is noise realization to be examined. For the sinograms, the covariance matrix K is diagonal, and was computed as $K_{ii} = (\bar{Y}_{1i} + \bar{Y}_{0i})/2$, which is acceptable if the signal is weak compared to the background. The signal-to-noise ratio (SNR) is estimated from the mean and variance of H_0 over multiple noise realizations.

In addition, three different reconstructions were computed. For each of them, a non-prewhitening observer was defined as follows:

$$H_n = (\bar{\lambda}_1 - \bar{\lambda}_0)^t \lambda, \quad (2)$$

where $\bar{\lambda}_1$ and $\bar{\lambda}_0$ are the expected reconstructions in the presence and absence of the signal, and λ is the reconstruction of a particular noise realization, and n indicates the reconstruction algorithm.

The first reconstruction algorithm was ML (expectation-maximization, 160 iterations, accelerated using a decreasing number of subsets), followed by post-smoothing with a 2D Gaussian. Different filter sizes were used.

TABLE I

THE MAXIMUM SNR FOR THE FOUR REGIONS FOR POST-SMOOTHED ML, FOR MAP AND FOR ML WITH POST-PROCESSING BASED ON THE PRIOR.

ROI	ideal	ML	MAP	pp-ML
0	6.2	5.7	5.6	4.6
1	6.3	6.1	5.9	4.7
2	6.4	5.5	5.5	5.1
3	7.5	6.5	6.9	5.7

The second reconstruction algorithm was MAP (same iteration scheme), which was previously described in [4]. This algorithm uses a position dependent prior. For the “gray matter” (white in figure 1), a Gibbs prior penalizing relative differences between neighboring pixels is applied [5]. In the two other anatomical regions (gray and black in figure 1), a Gaussian intensity prior is applied, where the mean of the Gaussian is estimated by maximizing the posterior. This posterior function has no local maxima. For this study, we assumed that the anatomical labels were unambiguous, no partial volume effects were taken into account.

The third algorithm attempts to incorporate the a-priori knowledge into the unsmoothed ML reconstruction (160 iterations). This is done by combining the prior described above with a Gaussian likelihood function defined as:

$$L = \sum_j (m_j - \lambda_j)^2, \quad (3)$$

where m_j is the (unsmoothed) ML value for pixel j , and λ_j is the pixel value being calculated. The likelihood L imposes similarity to the ML image, the prior suppresses noise, avoiding smoothing over anatomical edges. This procedure allows us to use the same prior function as a penalty and as a post-processing method.

III. EXPERIMENTS

Five sinograms were computed: one with normal activity, and one with a 20% decrease of activity in each of the four regions indicated in figure 1. For each of those, 100 noise realizations were computed. For each noise realization, the output of the ideal observer was computed, and multiple reconstructions with each of the three algorithms were made. For ML, the width of the Gaussian kernel was varied. For the two algorithms using the prior, the weight of the prior was varied. A wide range of the parameters was chosen such that an estimate of the maximum SNR could be obtained.

For each region, and for each reconstruction algorithm (and for each of its parameters), the non-prewhitening observer was computed using the reconstructions of the noise-free sinograms with and without signal, as described above. The SNR was computed from the mean and variance of the observer output for the 100 noise realizations.

IV. RESULTS

The estimate for the maximum SNR for each of the algorithms is tabulated in table I. With 100 noise realizations, the error on the standard deviation is about 15%.

V. DISCUSSION

If no a-priori knowledge is available, the SNR achieved by the ideal observer is an upper limit for any algorithm. The SNR of post-smoothed ML is relatively close to this upper limit. This SNR was obtained with a Gaussian kernel of full width at half maximum of 4 to 6 pixels.

Because the MAP algorithm uses additional information, one might hope to achieve an SNR which is even better than that of the ideal observer. In this simulation, the information loss due to reconstruction was apparently higher than the amount of information provided by the prior. The difference between post-smoothed ML and MAP is small, 100 realizations is not enough to rank the algorithms. This indicates that the prior supplies only a small amount of information about presence or absence of the signal. However, the MAP and ML images are very different and human observers may perform differently. For MAP, the best SNR was obtained with the highest value of the prior, probably because this prior information was nearly exact.

The most important result is the relatively poor performance of post-processed ML. We attribute this poor performance to the strong (negative) covariances that exist between neighboring pixel values in the ML-image [6]. These covariances also exist near edges, implying that pixel values in one anatomical region carry information about values in another region. The post-processing method carefully avoids any interaction between pixels from different anatomical regions. As a result, the information present in these neighboring pixels is lost. In contrast, simple post-smoothing combines pixels of different anatomical regions, making more information available to the non-prewhitening observer. If the anatomical prior is applied during reconstruction, the neighboring pixels of different anatomical regions can “exchange” information via the likelihood term (because the likelihood and its gradient are a function of all pixel values).

VI. CONCLUSION

Based on our simulation results, we hypothesize that for applications involving anatomical priors, penalized-likelihood reconstruction is superior to post-processed ML reconstruction.

REFERENCES

- [1] JW Stayman, JA Fessler, “Compensation for nonuniform resolution using penalized-likelihood reconstruction in space-variant imaging systems,” submitted to *IEEE Trans Med Imaging*.
- [2] J Nuysts, JA Fessler, “A penalized-likelihood image reconstruction method for emission tomography, compared to post-smoothed maximum-likelihood with matched spatial resolution.” *IEEE Trans Med Imaging*, in press.
- [3] HH Barrett, J Yao, JP Rolland, KJ Myers. “Model observers for assessment of image quality”. *Proc Natl Acad Sci USA* vol 90, pp 9758-9765, 1993.
- [4] K Baete, J Nuysts, W Van Paesschen, P Suetens, P Dupont. “Anatomical based FDG-PET reconstruction for the detection of hypometabolic regions in epilepsy.” *Proceedings of the IEEE NSS and MIC*, November 10-16, 2002, Norfolk, VA, USA.
- [5] J Nuysts, D Bequé, P Dupont, L Mortelmans. “A concave prior penalizing relative differences for maximum-a-posteriori reconstruction in emission tomography.” *IEEE Trans Nucl Sci*, vol 49, pp 56-60, 2002.
- [6] J Nuysts. “On estimating the variance of smoothed MLEM images.” *IEEE Trans Nucl Sci*, vol 49, pp 714-721, 2002.